Science of the Total Environment 860 (2023) 160489

Contents lists available at ScienceDirect

Science of the Total Environment

journal homepage: www.elsevier.com/locate/scitotenv

Buoyant microplastics in freshwater sediments – How do they get there?

Marziye Molazadeh [a,*], Fan Liu [a], Laura Simon-Sánchez [b], Jes Vollersten [a]

[a] Aalborg University, Section of Civil and Environmental Engineering, Department of the Built Environment, Thomas Manns Vej 23, 9220 Aalborg Øst, Denmark
[b] Institute of Environmental Science and Technology (ICTA-UAB), Universitat Autònoma de Barcelona, 08193 Cerdanyola del Vallès, Barcelona, Spain

HIGHLIGHTS

- MP content in the pond sediments varied up to two orders of magnitude.
- Buoyant MPs made up 95.4 % of the MP-mass and 83.5 % of the MP-number.
- No trend in the spatial distribution of MPs – neither concentration, size, nor polymer
- Mixing is an important factor for transporting buoyant MPs to the pond sediments.
- Sediment contents of silt and organic matter correlate with the MP-distribution.

GRAPHICAL ABSTRACT

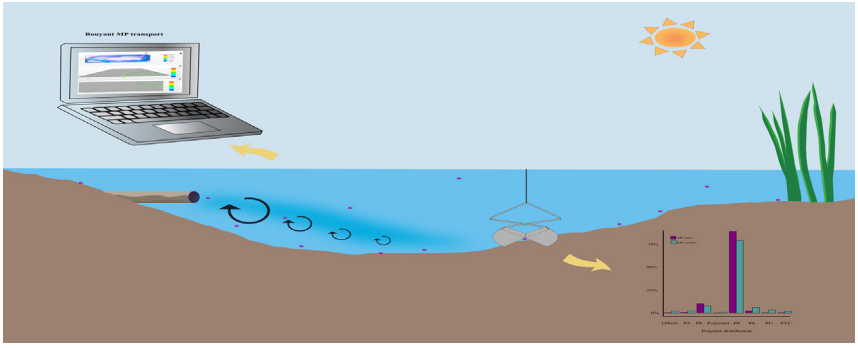

ARTICLE INFO

Editor: Dimitra A Lambropoulou

Keywords:
Buoyant MPs
Stormwater ponds
Sediments
CFD

ABSTRACT

The accumulation of microplastics (MPs) in the sediments of a stormwater treatment pond was studied to gain knowledge on how these facilities protect the natural environment against this emerging pollutant. Thirteen sediment samples were analyzed for MPs down to 10 μm, mapping the pattern of accumulation in the pond. The average abundance in terms of MP-number and mass was 11.8 μg kg^{-1} and 44,383 item kg^{-1}, respectively. They were rather unevenly distributed, with concentrations varying up to two orders of magnitude within the pond, showing that a trustworthy quantification of MPs retained by such units must rely on many and well-distributed subsamples. Buoyant MPs made up 95.4 % of the MP-mass and 83.5 % of the MP-number and in most of the sampled locations, polypropylene dominated the polymer fingerprint, followed by polyethylene. No spatial pattern in the distribution of MPs in the pond was identified. Instead, the MP content correlated to the organic matter and silt content, indicating that the processes leading to deposition could be similar. A computational fluid dynamics model was set up and used to simulate the transport mechanisms governing the conveyance of MPs in the pond from water to sediments. The results showed that the combination of advection and dispersion were likely the driving mechanism for buoyant (and non-buoyant) MPs to get in contact with the sediment bed and spread over the pond. Once in contact with the sediments, the MPs would have some probability of being permanently incorporated and hereby preventing them from entering the downstream aquatic environment.

1. Introduction

Plastics are an inevitable part of the modern world, and today's humans depend extensively on plastics for commercial, industrial, medical, and municipal applications. However, the ever-increasing production and use of plastic products has also paved the way for them to become serious environmental pollutants. The bulk of the plastic produced each year is used to make single-use products like disposable packaging or other short-lived items that are discarded within a year of manufacture (Hopewell et al., 2009). It is estimated that worldwide only 9 % of the plastic ever made is recycled and 12 % incinerated (Geyer et al., 2017). The rest is disposed of

* Corresponding author.
E-mail address: marziyem@build.aau.dk (M. Molazadeh).

http://dx.doi.org/10.1016/j.scitotenv.2022.160489
Received 8 August 2022; Received in revised form 17 November 2022; Accepted 21 November 2022
Available online 28 November 2022

at landfills or mismanaged, ending up in natural habitats. Despite the high persistence of synthetic polymers, large plastic items eventually fragmentate, mainly because of weathering caused by exposure to solar ultraviolet radiation and gradual loss of weight due to physical damage (Andrady, 2011). This degradation produces microplastics (MPs), commonly defined as plastic particles smaller than 5 mm in size (Arthur et al., 2009). Plastic particles which are derived from fragmentation of larger plastic items are commonly termed secondary MPs. Some MP particles are intentionally manufactured, for example, for direct usage in cosmetics and abrasives, or as raw materials to produce larger plastic items. These are commonly defined as primary MPs (Cole et al., 2011).

MPs, whether they be primary or secondary ones, are detrimental to the environment since they can be associated with a wide range of pollutants and toxic substances either from their production process, due to their adsorption characteristics, or by ingestion throughout the food web (Besseling et al., 2019; Cole et al., 2011). Since most plastic is produced and used inland (Boucher et al., 2019), urban areas are identified as important contributors of MPs into the environment. MPs can be introduced into urban freshwater and marine systems from various sources and through diverse routes. Stormwater, wastewater, and combined sewer overflows are commonly considered significant potential sources, discharging MPs to water bodies in urban areas (Schernewski et al., 2020). Freshwater MPs can ultimately end up in oceans if effective mitigation measures are not taken.

Stormwater runoff can be quite polluted as it 'cleans' the city's surfaces of all sorts of dirt and debris. It collects soluble and particulate pollutants, including MPs, and conveys them to downstream environments. It is hence common to install stormwater treatment facilities to protect the aquatic ecosystems. Their purpose is to detain and treat wet weather runoff flows to prevent damaging recipient water systems by mitigating the peak flow (F. Li et al., 2019; Duan et al., 2016) and trapping incoming particles into their bottom sediments (Gu et al., 2016). Retainment of particles is considered the most important process in stormwater runoff pollution removal. However, when it comes to MPs, there is a lack of knowledge on the degree to which they are retained, and which mechanisms are involved, leading to an inability to quantify their efficiency towards MPs and an inability to optimize their design towards this pollutant. MPs cannot per se be expected to behave like the bulk of stormwater particles as these mainly consist of sand, silt, and clay mixed with some organic debris. MPs, comprising both buoyant and non-buoyant polymers, may follow different floating and settling patterns. They may also have different physical properties such as Zeta potential, which would affect flocculation and attachment to surfaces.

The variability of MP type and load on stormwater facilities mainly depends on the pluviometric regime and the urbanization characteristic of the catchment. To date, MPs in the sediments of stormwater ponds have only been documented in a few studies (Liu et al., 2019b; Olesen et al., 2019; Ziajahromi et al., 2020; Moruzzi et al., 2020; Lutz et al., 2021). The majority of these were of polymers lighter than water (Liu et al., 2019b; Olesen et al., 2019; Lutz et al., 2021) and cannot be expected to have sunken to the bottom. Other transport mechanisms must hence have been in play for these floating MPs to reach the sediments. Possible candidates for such mechanisms are the ballasting of particles by biofilm formation, aggregation with other stormwater non-buoyant particles, ingestion and excretion by aquatic biota, as well as turbulent transport. These mechanisms have been reported to affect sedimentation and accumulation of buoyant MPs in some systems under some conditions (Kooi et al., 2017; Olesen et al., 2019).

However, research providing fundamental knowledge on prevailing processes and mechanisms that govern the movement and transport of MPs from water to sediments of shallow water systems is surprisingly scarce, and the MP migration processes remain poorly understood. It is necessary to address these and understand how shallow water bodies act as sinks for microplastics to actively design technical solutions for MP pollution management such as stormwater ponds, and to assess the efficiency of existing systems. The knowledge is furthermore important when understanding how natural shallow water bodies act as sinks for microplastics.

It is the objective to contribute to fill the knowledge gap on how MPs are retained by ponds designed to treat stormwater runoff, hereby mitigating impacts on the natural environment. The approach is to investigate the distribution of MPs in the sediments of one such pond in terms of MP-mass and number concentration, size distributions, and polymer composition. The results are intended to inform future studies on how to consider spatial variability of MPs in stormwater pond sediments, for example when sampling to quantify pond retention efficiencies. The driving factors for the observed spatial patterns are evaluated, as is the relation to sediment characteristics. For this evaluation, a 3D computable fluid dynamics (CFD) model was set up to gain a fundamental understanding of buoyant MP particle transport from the water to the sediments. These findings are intended to shed light on some key aspects of (buoyant) MP motion and fate in shallow, highly dynamic water systems.

2. Material and methods

2.1. Sample collection

Thirteen sediment samples were collected in August 2020 from a stormwater pond in Aarhus, Denmark (Fig. 1), using a Van Veen grab sampler. The pond receives runoff from residential and commercial areas, and occasionally illicit discharges of wastewater. The pond has an average stormwater residence time of two weeks and was constructed in 2008. The samples were taken during one dry weather day with no rain occurring for more than two days prior to the sampling. From each grab of sediments, the top 5–8 cm were collected and stored in glass jars, resulting in 2–3 kg bulk sediments for each location. All jars were transported to the laboratory and stored at 4 °C until further analysis.

2.2. Physicochemical characteristics of sediments

The organic matter content of the sediments was measured as loss-on-ignition by heating the dried sediments to 550 °C for 4 h in a muffle furnace (ASTM, 2000). To determine the grain size distributions, sediments were first treated with hydrogen peroxide (H_2O_2) to remove organic matter and consequently avoid hindering the size classification process. The oxidation was done as described in Section 2.3. Sediments were then dried at 105 °C for 24 h and homogenized. Collected sediment samples were characterized and separated into five different size fractions: <2 μm (clay), 2–63 μm (silt), 63–200 μm (fine sand), 200–630 μm (medium sand) and 630–3500 μm (coarse sand). The grain size distribution of each sample was determined using sieves with different mesh sizes for sediments larger than 63 μm and a hydrometer test for sediments smaller than 63 μm (Asadi et al., 2019).

2.3. Microplastic extraction

The bulk sediment (2–3 kg) samples were homogenized and subsamples representing 1.5 kg wet weight were treated. The subsamples were divided into several smaller batches and pre-oxidized in 5 L beakers by gradually adding 50 % hydrogen peroxide (H_2O_2) and Milli-Q water to the sample. H_2O_2 was added to a maximum of 10 % final concentration. The samples were stirred while oxidizing. The oxidation was continued until no foaming occurred when adding hydrogen peroxide. This procedure was repeated in all the batches until all 1.5 kg of sediments had been oxidized. The resulting oxidized sediments were combined and wet sieved on a 2 mm stainless steel sieve (Retsch GmbH, Germany). The sieved samples (<2 mm) were transferred to covered crystallizing dishes and placed in an oven at 50 °C for 5 days. For every sample, a dried sediment subsample of 200 g was taken for MP extraction and underwent density separation. The MP abundance was normalized to a concentration based on this dry weight. The process was performed in a 2-L pear-shaped separation funnel containing a sodium polytungstate (SPT) solution of density 1.89 g cm^{-3}.

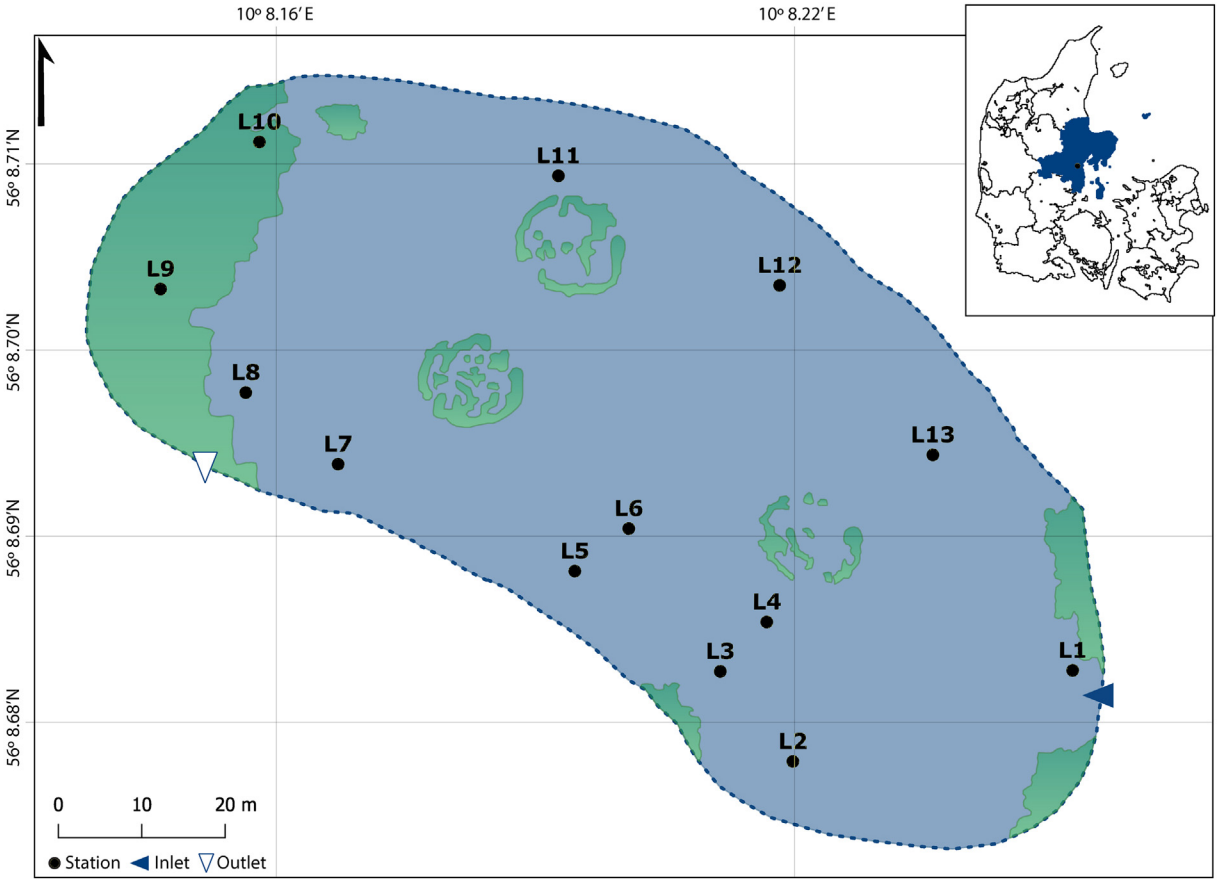

Fig. 1. Map of the pond showing the location of all the sampling stations. L stands for location. The green area in the left, where samples 9 and 10 were taken, is a shallow part of the pond with water depths about 0.2 m. The green areas in the centre (the circles) are areas with lower water depth (about 0.5 m) while the ones on the sides are some vegetation that has grown into the pond.

The mixture of sediments and SPT was aerated by compressed air from the bottom of the funnel for 30 min and left to settle for 24 h. Three-quarter of the bottom part was drained off and the floating particles collected and kept in a glass beaker. The process was repeated twice, meaning that the discarded part, which included the sediments, was collected and transferred back to the separation funnel and the whole process repeated to minimize the loss of particles in this step. The collected floating particles from both repetitions were filtered on a 10 μm steel filter. Subsequently, the filter was ultrasonicated to detach the particles and transfer them into a 300 mL sodium dodecyl sulfate solution (SDS, 5 % w/vol). The samples were incubated for 48 h at 50 °C and continuously mixed. The filtered particles went through enzyme purification steps with a blend of cellulase (Cellulase enzyme blend®, Sigma-Aldrich) and cellulolytic enzymes (Viscozyme®L, Sigma-Aldrich), again for 48 h at 50 °C, followed by protease, also at 50 °C for 48 h (Protease from Bacillus sp.®, Sigma-Aldrich) (Chand et al., 2022). A Fenton oxidation was performed by transferring the filtered particles into 200 mL of Milli-Q water and adding 145 mL of 50 % H_2O_2, 65 mL of 0.1 M NaOH, and 62 mL of 0.1 M $FeSO_4$ while maintaining the temperature at 15–30 °C. In order to separate larger particles (MP > 500 μm) from smaller ones (10 < MP < 500 μm), a 500 μm mesh sieve and a 10 μm stainless steel filter were used. The large particles retained on the sieve were collected and dried in an oven at 50–60 °C for later analysis. The smaller particles were transferred to a 250 mL separation funnel containing SPT (density of 1.89 g cm^{-3}) and the same separation procedure as previously described was performed. The particles were then filtered and collected into ultra-pure HPLC grade 50 % ethanol using an ultra-sonicating bath. The ethanol solution containing the particles was transferred to 10 mL vials and the ethanol evaporated in an evaporation bath (TurboVap® LV, Biotage) at 50 °C. Finally, the ethanol level in the vials was adjusted to 5 mL and particles were suspended in ultra-pure HPLC quality 50 % ethanol.

2.4. MP identification and quantification

Particles >500 μm suspected to be of plastic were manually sorted and imaged under a stereomicroscope (ZEISS, SteREO Discovery.V8, Oberkochen Germany). Particle dimensions were measured using ZenCore (Zen2Core SP1 from ZEISS) software. The particles were then analyzed by ATR-FTIR spectrometry (Cary 630, Agilent Technologies, with a single reflection diamond ATR). Interpretation of the particles' IR spectra was done using OMNIC software and its library (Thermo Fisher Scientific Inc., 8.2.0.387 version 1). However, particles above 1 mm in longest dimension were only occasionally detected in the samples and hence deemed outliers and not included in the study. Hence 1 mm was chosen as the upper size limit when reporting the data. For analyzing particles between 10 and 500 μm, FPA-μFTIR imaging was applied (Agilent Cary 620 FTIR microscope equipped with a 128 × 128 pixel FPA (Mercury Cadmium Telluride detector) and coupled to an Agilent 670 IR spectroscope). Sample deposition steps and instrument settings were similar to that of Chand et al. (2022) and Rasmussen et al. (2021). Briefly, a small sub-sample was taken of the particle suspension (the 5 mL of 50 % ethanol) using a glass pipette and deposited on a zinc selenide window (Ø13 × 2 mm, Crystran, UK) held in a compression cell with a Ø10 mm free area (Pike Technologies, USA). The window with its deposited particles was dried on a heating plate at 50 °C and the process repeated until the window was homogeneously covered by particles. Three windows from each sample were scanned. The resulting 3 × 3.2 million spectra from the scanning of the 10 × 10 mm area were processed applying the software siMPle, a software for

the automated detection of MP from μFTIR chemical imaging datasets (Primpke et al., 2020). siMPle analyses each individual spectrum by comparing it to a reference library and uses this to build images of MP particles (Liu et al., 2019a). The database used contained 124 reference spectra of plastics belonging to 35 polymer groups as well as natural organic materials, namely 7 groups which can be misinterpreted as plastics. The software provides particle dimensions, area, volume, and mass estimates of MPs (Primpke et al., 2020).

2.5. Contamination assessment

To avoid potential contamination during sample processing, all glassware and other equipment were rinsed three times with particle-free water and stainless-steel filters were muffled at 500 °C before use. Samples were covered with aluminium foils or glass watches during each treatment step. All liquid reagents were filtered through 0.7 μm glass fibre filters prior to use. Additionally, cotton lab coats were worn during all experimental steps. To minimize contamination from the ambient air, samples were processed inside a clean fume hood and the air in the FTIR and microscope lab room was continuously filtered with a Dustbox® (Hochleistungsluftreininger, Germany) holding a HEPA filter (H14, 7.5 m^2). Although many precautions were taken, contamination cannot be completely avoided. Considering this potential background contamination, three laboratory procedural blanks were analyzed in parallel with the samples. 200 g of muffled (500 °C) sediment surrogate, consisting of 75–1000 μm sand, was used for each blank. This amount is similar to the mass processed per sample. The blank control samples went through the same processes as the sediment samples. In the first iteration of using siMPle to identify MPs, an extraordinary amount of PP and PE particles were detected in some samples. The spectra of these suspicious particles were checked one by one, and many were found to be false positive identifications of some unknown natural material. To avoid these false positives, their spectra were included in the siMPle library as natural materials and assigned to a new group named 'fake particles'. Subsequently, all samples were analyzed again with the siMPle software using the new library. An example of these spectra is given in supplementary materials Fig. S1.

2.6. Statistical analysis

Statistical analyses were performed using R (version 3.5.3) and at a significance level of 0.05. The normality of the data was assessed by Shapiro-Wilks test. Kruskal-Wallis test was applied to investigate if there were differences in MP sizes and masses between different samples. Wilcoxon rank-sum test for pairwise comparisons was performed to compare the size and mass distribution of MP particles and identify those samples that differed significantly.

2.7. CFD simulations

The STARCCM + + commercial software was used to simulate flow fields. The particle tracking facility of the software was used to calculate MPs trajectories. For the continuous phase, a segregated flow model was used with the density of the fluid assumed constant. The fluid flow equations solved by the CFD model are based on the conservation of mass and momentum (Versteeg and Malalasekera, 1995). The flow was simulated as steady-state. All numerical simulations performed in this study solved the Reynolds-Averaged Navier-Stokes (RANS) equations with the k-ε (production and dissipation of turbulent kinetic energy) turbulence model. Details of the theoretical formulation can be found in the user guide of STARCCM + +. The inlet boundary condition was defined as velocity inlet corresponding to a storm condition with a relatively high inlet flow velocity. For the sloped walls and bottom of the pond, a non-slip wall condition was defined and the boundary condition for the outlet was assumed as a pressure outlet. The boundary condition for the water surface was set as a symmetry plane (Adamsson et al., 2005; Tamayol et al., 2010; Khan et al., 2013). The mesh sensitivity analysis of the results was performed by comparing velocities from the simulations with different numbers of meshes to ensure the solution was independent of mesh size and number. Four mesh densities were assessed: 14,586,364, 3,730,862, 1,892,719 and 1,101,167 cells. The number of 3,730,862 cells was found adequately fine and used in the subsequent analysis.

The Lagrangian Multiphase approach named 'particle tracking', was chosen to model the dispersed phase (i.e., MPs). A one-way coupling (uncoupled) approach between the flow field and MP load was chosen.

Several scenarios with varying inlet velocity, particle sizes and material densities were simulated, leading to similar conclusion thus one example is illustrated. In the example model the particles were modelled as spherical solids of 100 μm diameter and 900 g cm^{-3} density. To model particle dispersion, the effect of the fluid turbulence on the particle motion, the turbulent dispersion model was activated. Drag, gravitation, and buoyancy are the dominant forces exerted on the particles by the surroundings, including the continuous phase. These forces were included in the model. The drag coefficient was modelled using the Schiller-Naumann correlation. The boundary condition for the Lagrangian phase was assigned to 'escape' for all walls, meaning that once a MP hit the pond bottom or a wall, it was removed from the simulation.

3. Result and discussion

3.1. MP abundance

MPs were abundant in the pond with a global average for the 13 samples of 44,383 item kg^{-1} and 11.8 mg kg^{-1} of dry sediments (Table S1). The blank contamination was low compared to the measured concentrations with the highest contamination accounting for 0.1 % of the averaged measured value in terms of MP number concentration and 0.003 % in terms of MP mass concentration. Due to the low contamination compared to the MP abundance, the results were not corrected for contamination. A detailed description of MP contamination in blanks is given in supplementary materials in the section "MPs in blanks in supplementary file".

Comparing to other studies, our findings were lower than those of Olesen et al. (2019), who found 401.5 mg kg^{-1} and 9.5 × 10^5 item kg^{-1} in the sediments of a stormwater pond in Denmark. That pond was constructed in 1993 and dredged 10–15 years before sampling. It is in same region of Denmark as our pond and experiences similar climate conditions including rainfall patterns. The same goes for the seven stormwater retention ponds investigated by Liu et al. (2019b), which were constructed between 2005 and 2009. One of those ponds was the same as in the current study (termed C1 in their study). For that pond, they found approx. 2 times lower MP number and mass concentrations, even though they applied a quite similar sample purification and analysis approach. However, their sediment sample 'only' comprised three grab samples which were combined before analysis, whereas our study collected and analyzed thirteen separate samples from various positions in that pond. A likely explanation is hence sampling uncertainty caused by the high spatial variation in the pond (Table S1 in the supplementary materials, details in Section 3.2).

The MP concentrations extracted from sediments of a Gold Coast (Australia) stormwater wetland (Ziajahromi et al., 2020) and five open stormwater drainage systems in Australia (Lutz et al., 2021) were also lower than the average MP concentration detected in the present work. Ziajahromi et al. (2020) reported an average of 595 ± 120 item kg^{-1} dry sediment at the pond inlet and 320 ± 42 item kg^{-1} at its outlet. The mean concentration quantified by Lutz et al. (2021) for the five drainage systems was 664 item kg^{-1}. Other factors than inhomogeneity in the spatial distribution of MP can have led to the differences among the studies. One is that loadings from the catchment might differ due to land use, climate conditions such as rainfall patterns and amounts, and hydraulic loading (catchment impervious area per pond surface area, m^2/m^2). Age and hereby time for accumulation of MP might also have differed. Another possibility is that sample preparation can differ, where differences in filter mesh sizes, specific density of liquids used for density separation, and protocols for removal of organic material can lead to differences in extracted

MP. Once extracted, the instrument used for chemical quantification of extracted samples makes a difference on which MP polymer types can be identified and to what size they can be quantified (Primpke et al., 2020a,b). How much of a difference can be attributed to the analytical method is unclear, but several orders of magnitude have been reported (Lv et al., 2019), and it seems likely that this is one of the major reasons for the observed differences between studies.

MPs were assigned to six commonly used size fractions (Fig. 2) (Peng et al., 2017; Zheng et al., 2020; Liu et al., 2021). Most of the identified MPs, 4130 particles or 72.3 %, were in the size range of 10–100 μm. However, they contributed only 3.4 % to the total mass. Conversely, few large-sized particles (93 MPs of 500–1000 μm) constituted 50.4 % of the mass. MP abundance decreased as size increased (Fig. 2A), an observation which has also been made in other MP studies (Liu et al., 2019b).

The μFTIR analysis identified MPs belonging to 18 of the 35 addressed polymer types. Among these, 11 types were identified only in low amounts, accounting for 0.5 % and 2.2 % of MPs mass and number concentrations, respectively. These were assigned to a group termed 'Others'. Details regarding these polymers can be found in the supplementary materials (Table S2). Overall, the sum of the buoyant polymers (Polyethylene (PE): 0.9 g m^{-3}, Polypropylene (PP): 0.9 g m^{-3}) comprised 95.4 % and 83.5 % of mass and number of the identified MPs in the sediments. The water phase of same pond was studied by Liu et al. (2019a) who found that PP and PE together constituted >95 % of both the MP mass and number in the pond water.

PP was the dominant polymer, making up 85.6 % and 76.0 % of MP mass and number concentrations, respectively. The second most abundant polymer was PE, followed by Polystyrene (PS) and Polyamide (PA) in terms of mass and number (Fig. 2B). Although the number of Polyurethane (PU) particles was higher than that of Polyvinyl chloride (PVC), PVC contributed more to the total mass of particles, which can be due to the lower density of PU particles compared to PVC ones. These results are in accordance with several recently reported studies, where PP and PE were predominant polymers in the sediments (Lutz et al., 2021; Liu et al., 2019b; He et al., 2020; Olesen et al., 2019; Fan et al., 2019; all covering freshwater systems). Finding high concentrations of PP and PE in the sediments can be associated with their widespread use, from food packaging to the automotive industry. However, these materials are buoyant and must hence have been conveyed to the pond sediments by other mechanisms than simple density settling. A discussion of such mechanisms is given in Section 3.3.

3.2. Spatial MP distribution

Spatial distribution of MPs in the pond showed no systematic trends in terms of neither number nor mass concentrations (Table S1 and Fig. 3A). L2 and L6 were respectively the least and the most polluted locations in terms of number even though they were not far apart. Considering mass concentration, the least and most polluted locations were L2 and L11, which were on each their side of the pond.

Ziajahromi et al. (2020) sampled sediments close to the inlet and outlet of an Australian wetland, reporting the lowest MP concentration (number) at the outlet. They ascribed this to faster settling of high-density polymers and biofouling-assist settling of low-density polymers, albeit with no experimental verification hereof. It should be noted that the authors restricted their sampling to two locations (inlet and outlet), limiting the statistical strength of their statement.

The polymer composition at sampling sites did not follow a clear trend across the pond. Buoyant MPs, and especially those of PP, dominated at nearly all locations, both in terms of mass and number (Fig. 4A). PE was also common at all locations, albeit to a lesser degree. With respect to the non-buoyant polymers, polystyrene, polyamide (PA), polyurethane (PU), and PVC occurred at significant concentrations. The fact that both negatively and positively buoyant MPs were found reflect that the transport mechanism to the sediments was not simple sedimentation in calm water, but that the deposition was governed by some other mechanism.

For all sampling locations, the largest number of MPs were in the finest fraction (10–100 μm) and the lowest number in the coarsest fraction (500–1000 μm), which agrees with many previous studies, for example Kooi et al. (2021) who used a similar analytical technique as in the present study to characterize >60,000 MPs from different aquatic compartments and how they distributed in terms and size and other parameters. While the highest particle counts were found in the finest fraction, it only represented a minor contribution to the total mass (Fig. 4B), which is in line with what for example Huber et al. (2022) addressed for degradation of polypropylene from packaging materials and what Rasmussen et al. (2021) reported for raw wastewater.

The size and mass distribution of particles in each sample are illustrated in Fig. S2A, B and Table S3. No clear trend of size distribution versus location in the pond could be identified. This conclusion was confirmed by comparing the size distribution at all sites applying a non-parametric Kruskal-Wallis test (as data were not normally distributed as tested by a Shapiro-Wilk normality test). While the size distribution at some sites differed significantly ($p < 0.05$) from some others, the location of these sites showed no clear trend. Moreover, some sites, regardless of their locations, revealed a similar distribution of individual particles size ($p > 0.05$) (Table S4). Likewise, the mass of particles followed similar behavior to size (Table S5). In other words, the chance of finding a MP of a certain mass or size at a certain location in the pond did not show a systematic trend. The seeming randomness of the distribution of MPs in the sediments implies that the phenomena leading to their entrapment are complex. Gu et al. (2016) pointed out that a wide range of factors such as wind, vegetation, inflow patterns, construction of the outlet, turbulence levels, and

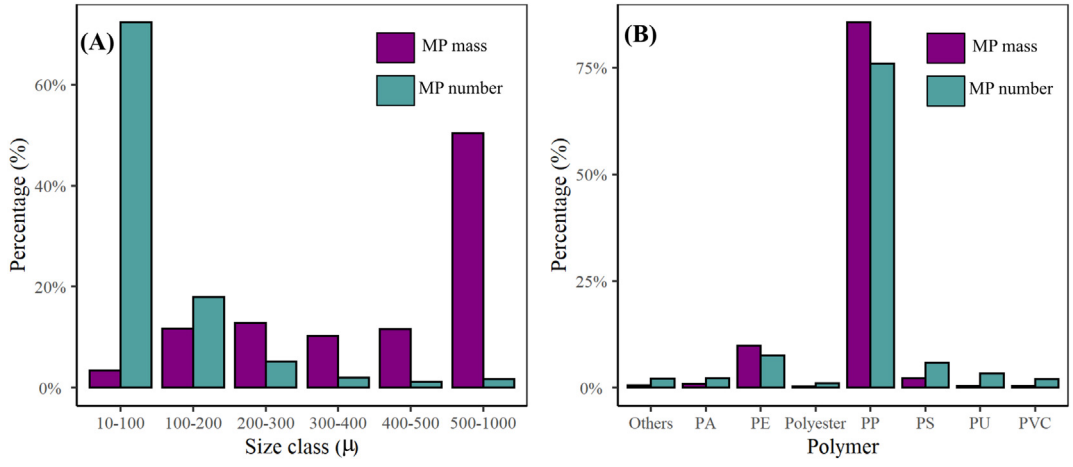

Fig. 2. MP percentage in each size class (A) and polymeric composition (B) of identified particles in terms of MP mass and number concentration.

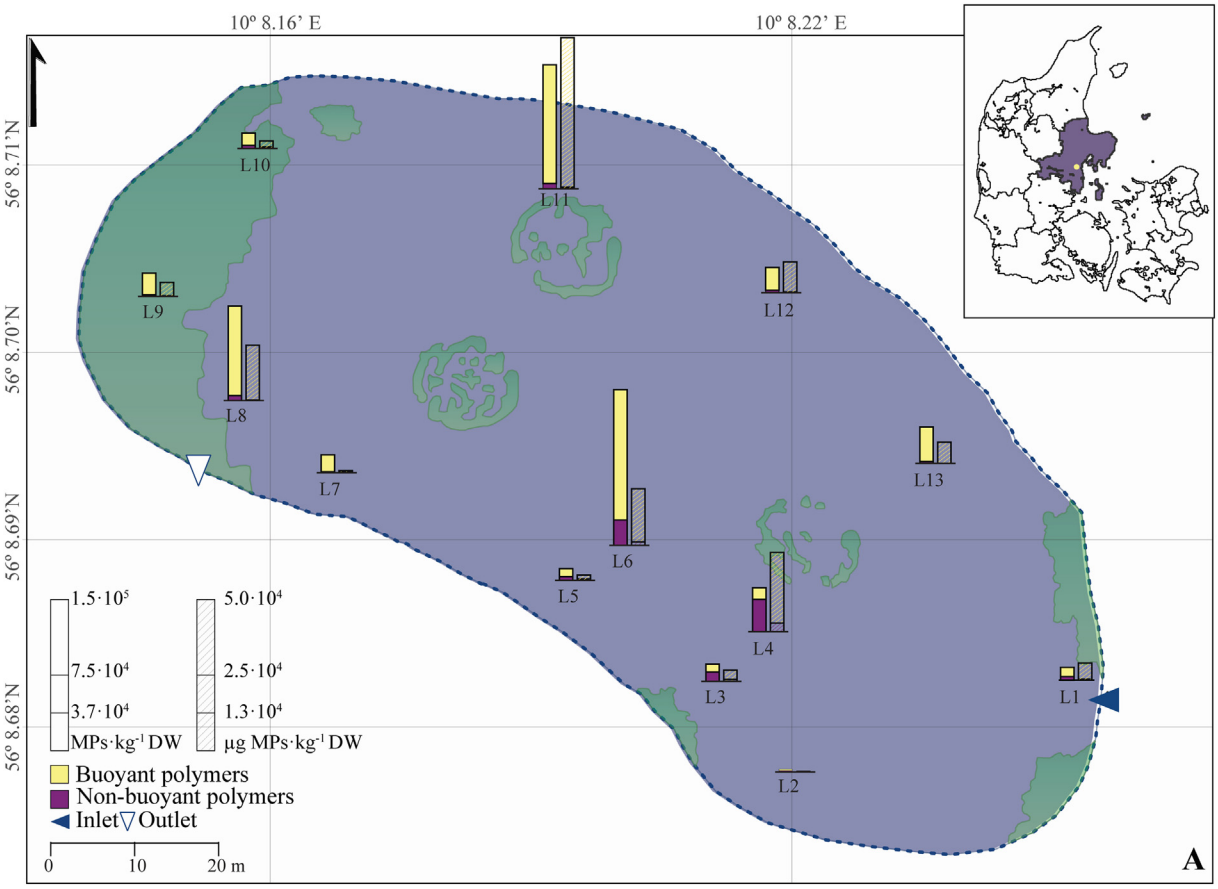

Fig. 3. Map showing the spatial distribution of MPs in terms of mass and number over the pond.

more, cannot be neglected when trying to conceptualize how particles are retained in a stormwater pond. It seems likely that the reason for the seemingly random distribution of MPs in the sediments of the studied pond is linked to such phenomena.

Contrary to our findings, Besseling et al. (2017), and using a hydraulic modelling approach to estimate the fate of non-buoyant micro- and nanoplastics, found that MP accumulation sites were dependent of particle size and argued that large-sized MP particle must be more abundant upstream than downstream, since they settle faster. This difference in findings can be due to gravimetric settling not being the main driving process for conveying MPs, especially the buoyant ones, from the water column to the sediments.

While there was no clear trend of where the MPs ended up in the pond, there was a clear positive correlation between organic matter and MP content in terms of both number ($r = 0.77$, $p < 0.05$) and mass ($r = 0.65$, $p < 0.05$) concentrations (Figs. S3 and S4). A similar trend was observed for silt and MP number ($r = 0.64$, $p < 0.05$) as well as mass ($r = 0.56$, $p < 0.05$) concentrations. No correlation was seen between clay and MP nor sand and MP. These findings agree with several other studies, where Liu et al. (2021), Corcoran et al. (2020), and Liu et al. (2019b) all found that MP abundance in sediments correlated positively with organic matter content, and Falahudin et al. (2020) and Liu et al. (2021) found that MP correlated positively with the silt content of marine and river sediments, respectively. One reason might be that hydrophobic organic matter agglomerates with hydrophobic MPs (Mato et al., 2001; Hong et al., 2017). Moreover, while correlation does not necessarily imply causality, the fact that sediment MP contents correlated with silt and organic matter implies that the transport mechanisms causing differences in these parameters may also be related or even similar.

He et al. (2020), on the other hand, reported a positive correlation with the clay content of river sediments. However, F. Li et al. (2019) and Y. Li et al. (2019) showed that settling of low-density polymer particles was not affected by adding clay particles to the suspension. These contradictory findings across varied aquatic systems and conditions suggest that the occurrence of MPs in sediments cannot be simply predicted by only the composition of the sediments, but is influenced by other site-specific confounding factors, among them site-specific hydrodynamics.

3.3. Transport mechanisms

The finding that there was no systematic relationship between sampling location and MP characteristics in terms of mass, size, and polymer composition shows that simple gravimetric settling cannot explain how MPs end up in the sediments of the pond. The question hence arises what can explain the observed MP-distribution, especially the fact that most MPs in the sediments were buoyant. One mechanism can be ballasted sedimentation where non-buoyant biofilm forms on a buoyant MP, allowing the ballasted particle to settle. Flocculation with non-buoyant particles will have a similar effect. These processes are known to occur in the deeper waters of the marine environment (Semcesen and Wells, 2021). Biological uptake and excretion as part of a non-buoyant fecal pellet would lead to a similar phenomenon (Cole et al., 2016).

Another mechanism is that buoyant MPs can be trapped by downwards moving flow currents, for example induced by inflow or wind. When the buoyancy-induced rising velocity of a MP is small compared to the downwards velocity of the current, the MP is conveyed to deeper waters. In the marine environment, wind induced mixing can lead to buoyant MPs reaching tens of meters into the water column (Kukulka et al., 2012). In shallow waters, MP conveyed by such downwards flow currents would have some probability of encountering the sediment bed and adhere to it.

In stormwater ponds the water flow is intrinsically unsteady and turbulent because of mixing induced by factors such as wind, intermittent inflow,

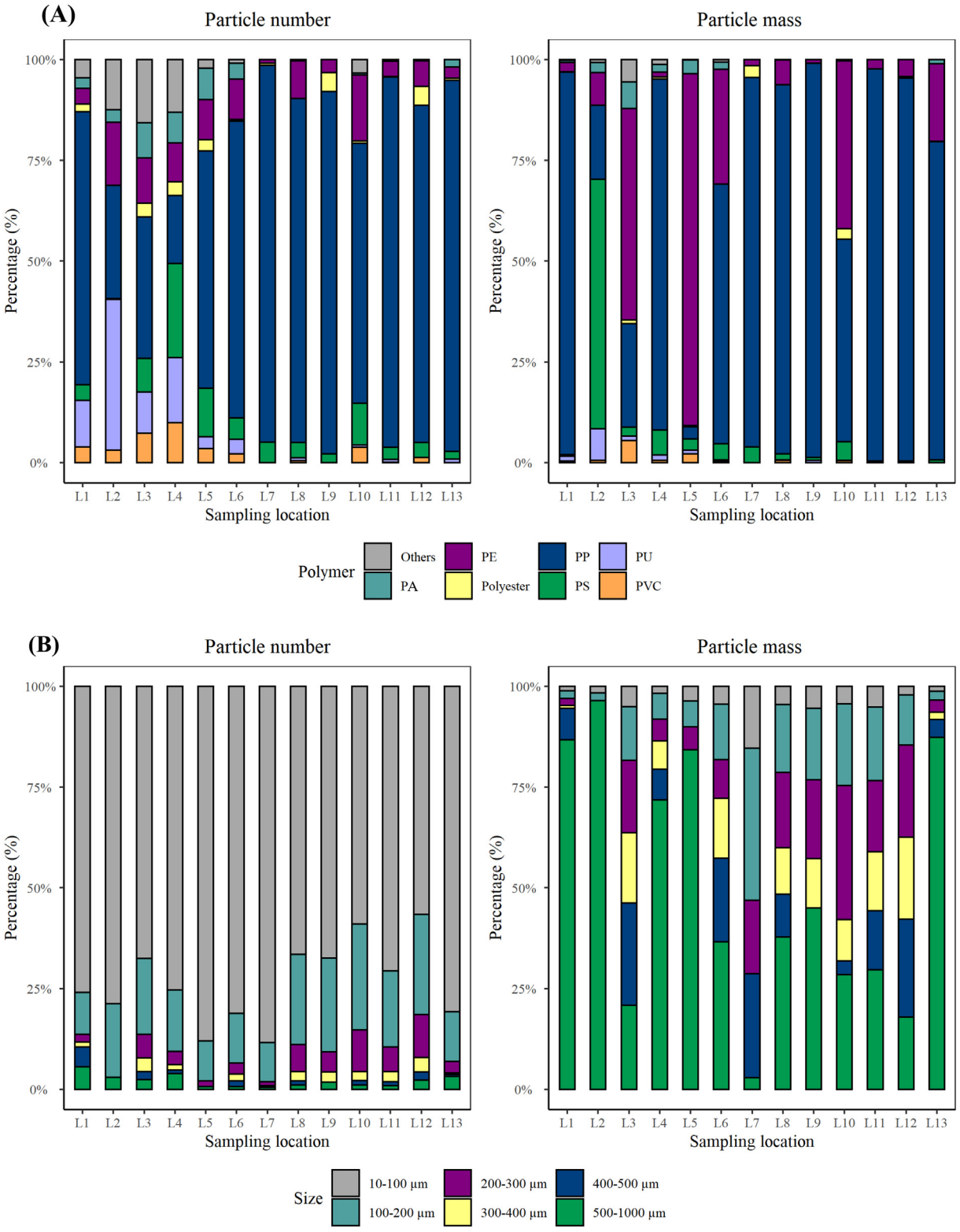

Fig. 4. Type distribution (A) and size distribution (B) of MPs identified at each sampling location based on particles number and mass.

diurnal temperature gradients, as well as their shallow depth (Hvitved-Jacobsen et al., 2010). The studied pond had a maximum depth of 1.2 m and wind induced mixing may lead to transport of MPs to its bottom, as wind over such water body can significantly affects its 3D flow pattern (Bentzen et al., 2008). Stormwater inflow can also introduce substantial mixing (Wium-Andersen et al., 2012), which might lead to similar transport processes. It hence seems reasonable to assume that downwards flow currents can convey MPs to the bottom of the pond where they may become trapped by the sediment bed.

To understand how downwards convective flow can lead to buoyant MPs reaching the sediment bed, particle trajectories were simulated with STAR-CCM+. The pond shape was simplified (Fig. 5) and downscaled 50

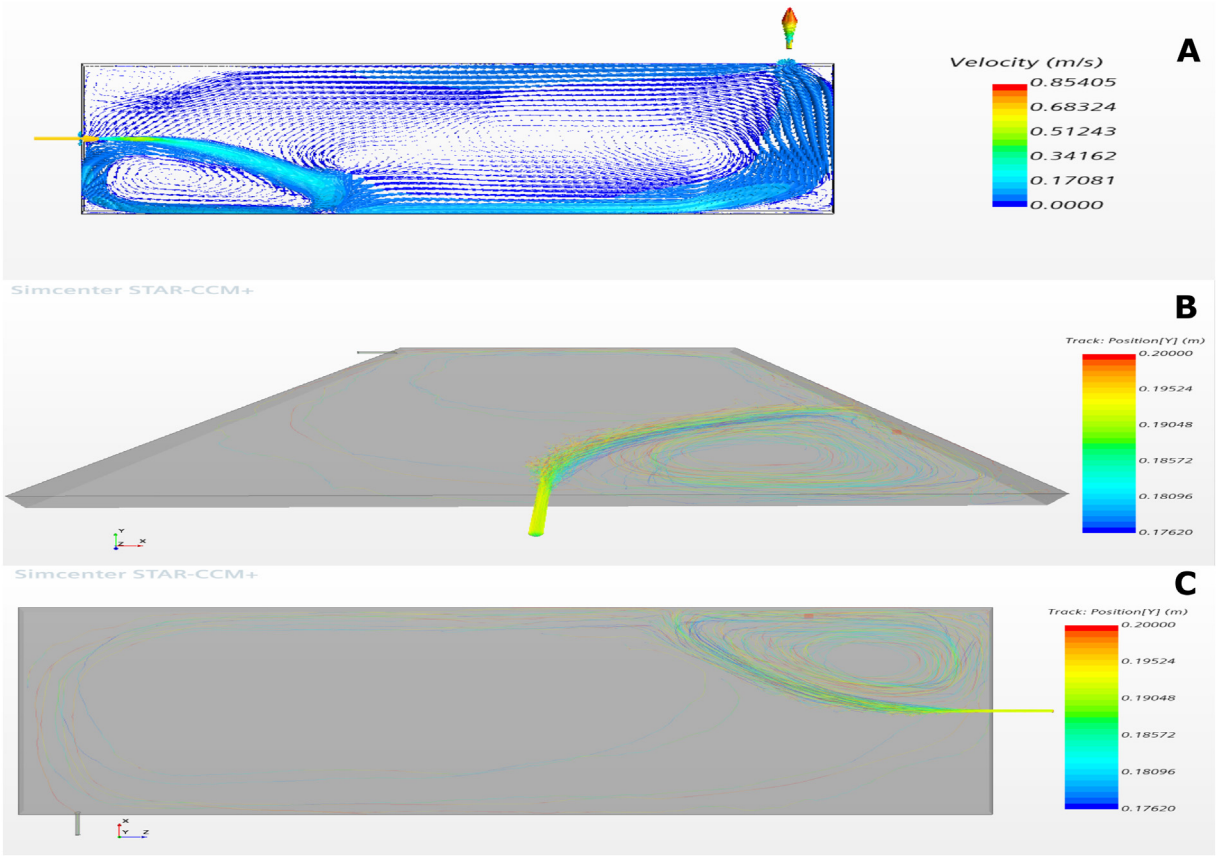

Fig. 5. Top view of velocity vectors indicating direction and magnitude of the flow velocity field for the modelled pond (A). Trajectories of the particles in the pond in 3D view (B), and top view (C). The trajectories are color-coded to show their z-position (dept below the water surface) in the flow field with respect to the corresponding particle position. Model particles were spheres of 100 μm diameter and 0.9 g cm^{-3} density.

times compared to the real one. Several scenarios were simulated, leading to similar conclusions: mixing-induced particle transport (dispersion) can explain why MPs – buoyant as well as non-buoyant – reach the sediment bed where they may become immobilized. To illustrate this, Fig. 5 shows a scenario where the inlet velocity was 0.7 m s^{-1} and spherical model particles of 100 μm diameter and 0.9 g cm^{-3} density were used as surrogates for buoyant MPs, corresponding to the particles having a Stokes settling velocity of $-5.4\ 10^{-5}$ m s^{-1}. Once a MP reached the sediment bed, it was simulated as being immobilized.

While biological and physio-chemical processes, e.g., biofilm growth and aggregation, may play a role in conveying buoyant MPs to the sediment bed of stormwater ponds they are hence strictly speaking not required to explain why these MPs accumulate in the pond sediments. Furthermore, biofilm growth is generally a slow process (Fazey and Ryan, 2016) and hence its effect might be small considering the typical water residence times in well-designed stormwater ponds (around 2 weeks, Hvitved-Jacobsen et al., 2010). Moreover, Besseling et al. (2017) in a modelling study found that the settling of MPs was rather unaffected by aggregation. It is hence quite possible that turbulent mixing (dispersion) is the governing processes for transporting small MPs from the water column of a stormwater pond, or a similar shallow water body, to its sediments.

The CFD modelling showed that the hydraulics were quite far from plug flow (Fig. 5A). The surface flow field in the pond mainly consisted of two asymmetry eddies (circulations), with the first clockwise in the lower-left corner and the second counterclockwise around the pond edge, forming a large stagnant zone at its centre. The trajectories of the MPs followed the same pattern as the flow (Fig. 5B). The color of the trajectories indicates the depth below the water surface, with the dark blue being the deepest. Once a particle hit the bottom, it was simulated sticking to it and hence retained by the sediments. The MP's downwards (or upwards) velocity caused by the eddies tended to be significantly above the numerical value of the settling (or rising) velocity. The particles hence followed the flow field. The simulations further showed that most particles sooner or later hit the bottom and hence were retained.

The simulation discussed above and shown in Fig. 5 is only one example of an indefinite number of possible configurations of pond shape, hydraulic conditions, MP size, MP density, MP shape, and so on. Nevertheless, it is a realistic one and as such shows that advective transport and dispersion can be an efficient mechanism to transport buoyant MPs to the pond bottom where they may stick to the sediments.

Other scenarios were simulated where the polymer density was modified to reflect phenomena like ballasting due to biofilm growth and non-buoyant polymers. These showed that capturing efficiency increased for non-buoyant particles as they had slightly different trajectories when the flow underwent acceleration in x, y, or z directions. I.e., when the flow lines bent because they got close to a surface such as the pond bottom. Here the inertia of the particles tended to keep them on a 'straighter' line pointing towards the surface, increasing the rate of hitting that surface compared to the buoyant ones. Examples of such simulations are shown in supplementary material, Fig. S5 and S6. Depending on density and size, particles travelled some distances before being immobilized by the pond bottom. The reason was that both buoyant and non-buoyant particles were conveyed by eddies and if the upward velocity component was larger than the settling velocity, they tended to follow the eddies until escaping them and their trajectory terminated (Figs. S5 and S6).

It must again be stressed that the above simulations are only a few among legion possible scenarios and that the model pond was strongly simplified compared to the real one. It furthermore ignores important aspects

such as resuspension of sediments, plant growth, variations in inflow, wind speed, wind direction, stratification, etcetera. The simulations hence solely yield a proof of concept that mixing due to for example inflow of stormwater can lead to a high fraction of buoyant particles in the inlet reaching the sediment bed. Where they in reality will end up and where they ultimately will accumulate cannot be predicted hereby. It can furthermore be argued that mixing may also lead to entrapment of buoyant MPs under other highly turbulent flows regimes, such as rivers, shipping fairways, and the upper layers of open waters, where dispersion (mixing) may govern the MP transport till the MPs reach the bottom of the water body or deeper zones where the flow is less turbulent or even laminar.

4. Conclusion

The MP-content of the 13 collected samples varied up to two orders of magnitude, illustrating that a simple grab sample in such pond is unlikely to be representative. The by far largest part of the MPs was buoyant with small-sized low density PP particles dominating at most locations. There was no trend of how MPs distributed in the pond, neither regarding masses, numbers, sizes, or polymer types. In other words, the spatial distribution of MPs was independent of MP properties. The findings consequently indicated that simple density driven settling in quiescent water, as for example described by Stokes Law, cannot explain how the MPs ended up in the sediments. The study also showed that there was statistically significant correlation between the content of MP, organic matter, and silt, but not between MP and clay, indicating that particles of natural organic matter, silt, and MP particles seemed to behave similar with respect to being immobilized in the pond sediments.

Computable fluid dynamics modelling allowed identifying a likely mechanism for transport of MPs – also the buoyant ones – from the water column to the sediments. In the shallow and highly dynamic water of the pond, the dominating mechanism for conveying MPs from the water column to the sediments and spread across the pond was advection combined with turbulent dispersion (mixing).

Once an MP reaches the sediments, it has some probability of being permanently immobilized by them. That probability will depend on local hydrodynamic condition and sediment physicochemical properties.

CRediT authorship contribution statement

Marziye (Shabnam) Molazadeh carried out the experiments and simulation, interpreted the results, and wrote the initial draft. Laura Simon-Sanchez drew the maps. Fan Liu contributed to the sampling and co-supervised the project. Jes Vollertsen supervised the project. All authors contributed to the final manuscript.

Data availability

Data will be made available on request.

Declaration of competing interest

The authors declare no competing interests.

Acknowledgements

This work was carried out within the Limnoplast project. This project has received funding from the European Union's Horizon 2020 research and innovation programme under the Marie Skłodowska-Curie grant agreement No 860720.

Appendix A. Supplementary data

Supplementary data to this article can be found online at https://doi.org/10.1016/j.scitotenv.2022.160489.

References

Adamsson, A., Bergdahl, L., Lyngfelt, S., 2005. Measurement and three-dimensional simulation of flow in a rectangular detention tank. Urban Water J. 2 (4), 277–287. https://doi.org/10.1080/15730620500386545.

Andrady, A.L., 2011. Microplastics in the marine environment. Mar. Pollut. Bull. 62, 1596–1605. https://doi.org/10.1016/j.marpolbul.2011.05.030.

Arthur, C., Baker, J.E., Bamford, H.A., 2009. Proceedings of the International Research Workshop on the Occurrence, Effects, and Fate of Microplastic Marine Debris, September 9-11, 2008. University of Washington Tacoma, Tacoma, WA, USA.

Asadi, A.M., Maizar, Hertika, S.A., Iranawati, F., Yuwandita, A.Y., 2019. Microplastics in the sediment of intertidal areas of Lamongan, Indonesia. Int. J. Bioflux Soc. 12, 1065–1073. http://www.bioflux.com.ro/aacl.

ASTM, 2000. Standard test methods for moisture, ash, and organic matter of peat and other organic soils. Method D 2974-00. American Society for Testing and Materials, West Conshohocken, PA 2000. American Society for Testing and Materials.

Bentzen, T.R., Larsen, T., Rasmussen, M.R., 2008. Wind effects on retention time in highway ponds. Water Sci.Technol. 57, 1713–1720. https://doi.org/10.2166/wst.2008.267.

Besseling, E., Quik, J.T.K., Sun, M., Koelmans, A.A., 2017. Fate of nano- and microplastic in freshwater systems: a modeling study. Environ. Pollut. 220 (A), 540–548. https://doi.org/10.1016/j.envpol.2016.10.001.

Besseling, E., Hasselerharm, P.R., Foekema, E.M., Koelmans, A.A., 2019. Quantifying ecological risks of aquatic micro- and nanoplastic. Crit. Rev. Environ. Sci. Technol. 49 (1), 32–80. https://doi.org/10.1080/10643389.2018.1531688.

Boucher, J., Faure, F., Pompini, O., Plummer, Z., Wieser, O., de Alencastro, L.F., 2019. (Micro) plastic fluxes and stocks in Lake Geneva basin. TrAC Trends Anal. Chem. 112, 66–74. https://doi.org/10.1016/j.trac.2018.11.037.

Chand, R., Kohansal, K., Toor, S., Pedersen, T.H., Vollertsen, J., 2022. Microplastics degradation through hydrothermal liquefaction of wastewater treatment sludge. J. Clean. Prod. 335, 130383. https://doi.org/10.1016/j.jclepro.2022.130383.

Cole, M., Lindeque, P., Halsband, C., Galloway, T.S., 2011. Microplastics as contaminants in the marine environment: a review. Mar. Pollut. Bull. 62, 2588–2597. https://doi.org/10.1016/j.marpolbul.2011.09.025.

Cole, M., Lindeque, K.P., Fileman, E., Clark, J., Lewis, C., Halsband, C., Galloway, S.T., 2016. Microplastics alter the properties and sinking rates of zooplankton faecal pellets. Environ. Sci.Technol. 50, 3239–3246. https://doi.org/10.1021/acs.est.5b05905.

Corcoran, P.L., Belontz, S.L., Ryan, K., Walzak, M.J., 2020. Factors controlling the distribution of microplastic particles in benthic sediment of the Thames River, Canada. Environ. Sci. Technol. https://doi.org/10.1021/acs.est.9b04896.

Duan, H.F., Li, F., Yan, H., 2016. Multi-objective optimal design of detention tanks in the urban stormwater drainage system: LID implementation and analysis. Water Resour. Manag. 30 (13), 4635–4648. https://doi.org/10.1007/s11269-016-1444-1.

Falahudin, D., Cordova, M.R., Sun, X., Yogaswara, D., Wulandari, I., Hindarti, D., Arifin, Z., 2020. The first occurrence, spatial distribution and characteristics of microplastic particles in sediments from Banten Bay, Indonesia. Sci. Total Environ. 705, 135304. https://doi.org/10.1016/j.scitotenv.2019.135304.

Fan, Y., Zheng, K., Zewen, Z., Guangshi, C., Peng, X., 2019. Distribution, sedimentary record, and persistence of microplastics in the Pearl River catchment, China. Environ. Pollut. 251, 862–870. https://doi.org/10.1016/j.envpol.2019.05.056.

Fazey, F.M.C., Ryan, P.G., 2016. Biofouling on buoyant marine plastics: an experimental study into the effect of size on surface longevity. Environ. Pollut. 210, 354–360. https://doi.org/10.1016/j.envpol.2016.01.026.

Geyer, R., Jambeck, J.R., Law, K.L., 2017. Production, use, and fate of all plastics ever made. Sci. Adv. 3. https://doi.org/10.1126/sciadv.1700782.

Gu, L., Dai, B., Zhu, D.Z., Hua, Z., Liu, X., Duin, B., Mahmood, K., 2016. Sediment modelling and design optimization for stormwater ponds. Can. Water Resour. J. 42 (1), 70–87. https://doi.org/10.1080/07011784.2016.1210542.

He, B., Goonetilleke, A., Ayoko, G.A., Rintoul, L., 2020. Abundance, distribution patterns, and identification of microplastics in Brisbane River sediments,Australia. Sci. Total Environ. 700, 134467. https://doi.org/10.1016/j.scitotenv.2019.134467.

Hong, S.H., Shim, W.J., Hong, L., 2017. Methods of analysing chemicals associated with microplastics: a review. Anal. Methods https://doi.org/10.1039/x0xx00000x.

Hopewell, J., Dvorak, R., Kosior, E., 2009. Plastics recycling: challenges and opportunities. Philos. Trans. R. Soc. B Biol. Sci. 364 (1526), 2115–2126. https://doi.org/10.1098/rstb.2008.0311.

Huber, M., Archodoulaki, V.M., Pomakhina, E., Pukanszky, B., Zinocker, E., Gahleitner, M., 2022. Environmental degradation and formation of secondary microplastics from packaging material: a polypropylene film case study. Polym. Degrad. Stab. 195, 109794. https://doi.org/10.1016/j.polymdegradstab. 2021.109794.

Hvitved-Jacobsen, T., Vollertsen, J., Nielsen, A.H., 2010. Urban and Highway Stormwater Pollution – Concepts and Engineering. CRC Press/Taylor & Francis Group. ISBN: 978-1-4398-2685-0, p. 347 https://doi.org/10.1201/9781439826867 (section 9.3.1.7).

Khan, S., Melville, B.W., ASCE, M., Shamseldin, A.Y., Fischer, C., 2013. Investigation of flow patterns in storm water retention ponds using CFD. J. Environ. Eng. 139, 61–69. https://doi.org/10.1061/(ASCE)EE doi:1943-7870.0000540.

Kooi, M., Besseling, E., Kroeze, C., Wenzel, A.P.V., Koelmans, A.A., 2017. Modeling the Fate and Transport of Plastic Debris in Freshwaters: Review and Guidance. Part of the Handbook of Environmental Chemistry Book Series. 58, pp. 125–152. https://doi.org/10.1007/978-3-319-61615-5_7.

Kooi, M., Primpke, S., Mintenig, S.M., Lorenz, C., Gerdts, G., Koelmans, A.A., 2021. Characterizing the multidimensionality of microplastics across environmental compartments. Water Res. 202, 117429. https://doi.org/10.1016/j.watres.2021.117429.

Kukulka, T., Proskurowski, G., Morét-Ferguson, S., Meyer, D.W., Law, K.L., 2012. The effect of wind mixing on the vertical distribution of buoyant plastic debris. Geophys. Res. Lett. 39. https://doi.org/10.1029/2012GL051116.

Li, F., Yan, X.F., Duan, H.F., 2019. Sustainable design of urban stormwater drainage systems by implementing detention tank and LID measures for flooding risk control and water quality management. Water Resour.Manag. 33 (9), 3271–3288. https://doi.org/10.1007/s11269-019-02300-0.

Li, Y., Wang, X., Fu, W., Xia, X., Liu, C., Min, J., Zhang, W., Crittenden, J.C., 2019. Interactions between nano/micro plastics and suspended sediment in water: implications on aggregation and settling. Water Res. 161, 486–495. https://doi.org/10.1016/j.watres.2019.06.018.

Liu, F., Olesen, K.B., Borregaard, A.R., Vollertsen, J., 2019a. Microplastics in urban and highway stormwater retention ponds. Sci. Total Environ. 671, 992–1000. https://doi.org/10.1016/j.scitotenv.2019.03.416.

Liu, F., Vianello, A., Vollertsen, J., 2019b. Retention of microplastics in sediments of urban and highway stormwater retention ponds *. Environ. Pollut. 255, 113335. https://doi.org/10.1016/j.envpol.2019.113335.

Liu, Y., Zhang, J., Tang, Y., He, Y., Li, Y., You, J., Breider, F., Tao, S., Liu, W., 2021. Effects of anthropogenic discharge and hydraulic deposition on the distribution and accumulation of microplastics in surface sediments of a typical seagoing river: the Haihe River. J. Hazard. Mater. 404 (B), 124180. https://doi.org/10.1016/j.jhazmat.2020.124180.

Lutz, N., Fogarty, J., Rate, A., 2021. Accumulation and potential for transport of microplastics in stormwater drains into marine environments, Perth region,Western Australia. Mar. Pollut. Bull. 68, 112362. https://doi.org/10.1016/j.marpolbul.2021.112362.

Lv, L., Yan, X., Feng, L., Jiang, S., Lu, Z., Xie, H., Sun, S., Chen, J., Li, C., 2019. Challenge for the detection of microplastics in the environment. Water Environ. Res. https://doi.org/10.1002/wer.1281.

Mato, Y., Isobe, T., Takada, H., Kanehiro, H., Ohtake, C., Kaminuma, T., 2001. Plastic resin pellets as a transport medium for toxic chemicals in the marine environment. Environ. Sci. Technol. https://doi.org/10.1021/es0010498.

Moruzzi, R.B., Speranza, L.G., Conceição, F.T.D., Martins, S.T.D.S., Busquets, R., Campos, L.C., 2020. Stormwater detention reservoirs: an opportunity for monitoring and a potential site to prevent the spread of urban microplastics. Water 12 (7), 1994. https://doi.org/10.3390/w12071994.

Olesen, K.B., Stephansen, D.A., van Alst, N., Vollertsen, J., 2019. Microplastics in a stormwater pond. Water (Switzerland) 11 (7), 1466. https://doi.org/10.3390/w11071466.

Peng, G., Zhu, B., Yang, D., Su, L., Shi, H., Li, D., 2017. Microplastics in sediments of the Changjiang Estuary, China☆. Environ. Pollut. 225, 283–290. https://doi.org/10.1016/j.envpol.2016.12.064.

Primpke, S., Cross, R.K., Mintenig, S.M., Simon, M., Vianello, A., Gerdts, G., Vollertsen, J., 2020. EXPRESS: toward the systematic identification of microplastics in the environment: evaluation of a new independent software tool (siMPle) for spectroscopic analysis. Appl. Spectrosc. 74, 1127–1138. https://doi.org/10.1177/0003702820917760.

Primpke, S., Christiansen, S.K., Cowger, W., Frond, H.D., Deshpande, A., Fischer, M., Holland, E.B., Meynes, M., O'Donnell, B.A., Ossmann, B.E., Pittroff, M., Sarau, G., Scholz-Bo¨ttcher, B.M., Wiggin, J.K., 2020. Critical assessment of analytical methods for the harmonized and cost-efficient analysis of microplastics. Appl. Spectrosc. 74, 1012–1047. https://doi.org/10.1177/0003702820921465.

Rasmussen, L.A., Iordachescu, L., Tumlin, S., Vollertsen, J., 2021. A complete mass balance for plastics in a wastewater treatment plant - macroplastics contributes more than microplastics. Water Res. 201, 117307. https://doi.org/10.1016/j.watres.2021.117307.

Schernewski, G., Radtke, H., Hauk, R., Baresel, C., Olshammar, M., Osinski, R., Oberbeckmann, S., 2020. Transport and behavior of microplastics emissions from urban sources in the Baltic Sea. Front. Environ. Sci. 8, 579361. https://doi.org/10.3389/fenvs.2020.579361.

Semcesen, O.P., Wells, G.M., 2021. Biofilm growth on buoyant microplastics leads to changes in settling rates: implications for microplastic retention in the Great Lakes. Mar. Pollut. Bull. 170, 112573. https://doi.org/10.1016/j.marpolbul.2021.112573.

Tamayol, A., Firoozabadi, B., Ashjari, M.A., 2010. Hydrodynamics of secondary settling tanks and increasing their performance using baffles. J. Environ. Eng. 136 (1), 32–39. https://doi.org/10.1061/(ASCE)EE.1943-7870.0000126.

Versteeg, H.K., Malalasekera, W., 1995. An Introduction to Computational Fluid Dynamics: The Finite Volume Method. Longman Scientific and Technical, New York, NY, USA.

Wium-Andersen, T., Nielsen, A.H., Hvitved-Jacobsen, T., Vollertsen, J., 2012. Modeling nutrient and pollutant removal in three wet detention ponds. In: Rauch, S., Morrison, G. (Eds.), Urban Environment. Alliance for Global Sustainability Bookseries 19. https://doi.org/10.1007/978-94-007-2540-9_22.

Zheng, Y., Lia, J., Cao, W., Jiang, F., Zhao, C., Ding, H., Wang, M., Gao, F., Sun, C., 2020. Vertical distribution of microplastics in bay sediment reflecting effects of sedimentation dynamics and anthropogenic activities. Mar. Pollut. Bull. 152, 110885. https://doi.org/10.1016/j.marpolbul.2020.110885.

Ziajahromi, S., Drapper, D., Hornbuckle, A., Rintoul, L., Leusch, F.D.L., 2020. Microplastic pollution in a stormwater floating treatment wetland: detection of tyre particles in sediment. Sci. Total Environ. 713, 136356. https://doi.org/10.1016/j.scitotenv.2019.136356.